

# The Distribution of Dark Matter in Galaxies: the Core Radius Issue

Paolo Salucci<sup>1</sup>

SISSA, Via Beirut, 2-4 I-34014 Trieste, Italy, [salucci@sissa.it](mailto:salucci@sissa.it)

**Abstract.** I review the up-to-date status on the properties of the Dark Matter density distribution around Galaxies. The rotation curves of spirals all conform to a same Universal profile which can be uniquely decomposed as the sum of an exponential thin stellar disk and a dark halo with a flat density core. From dwarfs to giants galaxies, the halos embedding the stellar component feature a constant density region of size  $r_0$  and value  $\rho_0$ , which are inversely correlated. The fine structure of dark halos in the region of the stellar disk has been derived for a number of low-luminosity disk galaxies: the halo circular velocity increases almost linearly with radius out to the edge of the stellar disk, implying, up there, an almost constant dark matter density. This sets a serious discrepancy between the cuspy density distribution predicted by N-body simulations of  $\Lambda$ CDM cosmology, and those actually detected around galaxies.

The small scatter around the Fundamental Plane (FP) of elliptical galaxies constraints the distribution of dark and luminous matter in these systems. The measured central velocity dispersion  $\sigma_0$  in the FP is linked to both photometric and dynamical properties of luminous and dark matter. As a consequence, the well-known features of the FP imply that, inside the effective radius  $R_e$ , the stellar spheroid must dominate over the dark matter, in contrast with  $\Lambda$ CDM predictions.

## 1 Introduction

Rotation curves (RC's) of disk galaxies are the best probe for dark matter (DM) on galactic scale. Notwithstanding the impressive amount of knowledge gathered in the past 20 years, only very recently we start to shed light on crucial aspects of the mass distribution of Dark Matter in galaxies, including its radial density profile, and its Universality.

On a cosmological side, high-resolution N-body simulations have shown that cold dark matter (CDM) halos achieve a specific equilibrium density profile [13 hereafter NFW, 5, 8, 12, 9] characterized by one free parameter, e.g. the halo mass. In the innermost region, the DM halo density shows an average profile which is characterized by a power-law cusp  $\rho \sim r^{-\gamma}$ , with  $\gamma = 1 - 1.5$  [13, 12, 2]. In detail, CDM halos have:

$$\rho_{\text{NFW}}(r) = \frac{\rho_s}{(r/r_s)(1 + r/r_s)^2} \quad (1)$$

where  $r_s$  and  $\rho_s$  are respectively the characteristic inner radius and density. Let us define  $r_{\text{vir}}$  as the radius within which the mean density is  $\Delta_{\text{vir}}$  times the mean

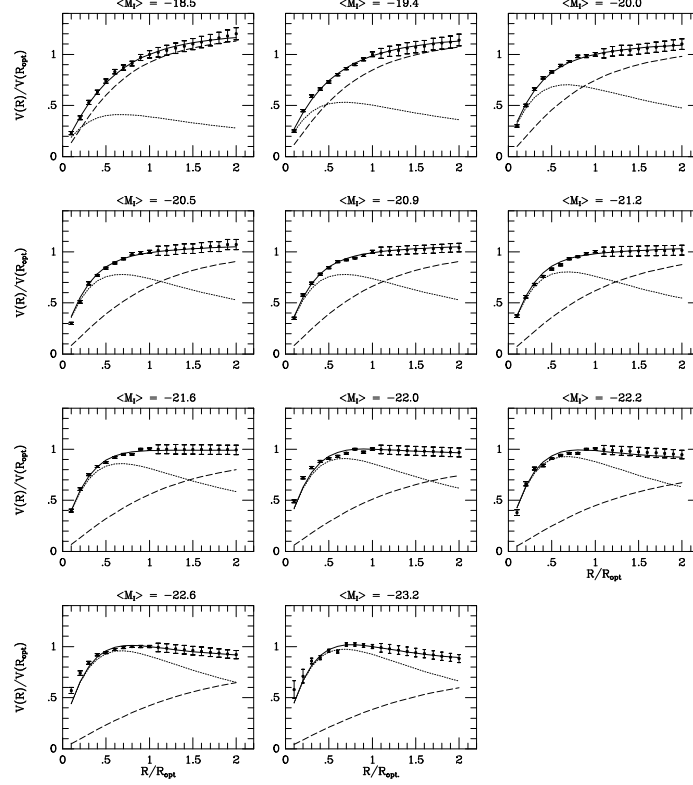


**Fig. 1.** Synthetic rotation curves (filled circles with error bars) and the Universal Rotation Curve (solid line). The separate dark/luminous contributions are indicated by a dotted line (disk) and a dashed line (halo).

universal density  $\rho_m$  at the halo formation redshift, the associated virial mass as  $M_{\text{vir}}$  and the halo velocity as  $V_{\text{vir}} \equiv GM_{\text{vir}}/r_{\text{vir}}$ . In the "concordance"  $\Lambda$ CDM scenario:  $\Omega_m = 0.3$ ,  $\Omega_\Lambda = 0.7$  and  $h = 0.7$ , so that  $\Delta_{\text{vir}} \simeq 340$  at  $z \simeq 0$ . Let us set  $c \equiv r_{\text{vir}}/r_s$ , and from simulations  $c \simeq 21(M_{\text{vir}}/10^{11})^{-0.13}$ , then in CDM framework circular velocity of dark halos  $V_{\text{NFW}}(r)$  depends only on their virial masses and takes the form:

$$V_{\text{NFW}}^2(r) = V_{\text{vir}}^2 \frac{c}{A(c)} \frac{A(x)}{x} \quad (2)$$

where  $x \equiv r/r_s$  and  $A(x) \equiv \ln(1+x) - x/(1+x)$ .

From the observational point of view, only recently the difficulties in deriving the internal structure of halos from available kinematics have been overcome. This has been done *i)* by means of a careful study of the Universal Rotation Curve [16] built out of 1000 individual RC's, *ii)* by adopting an halo velocity

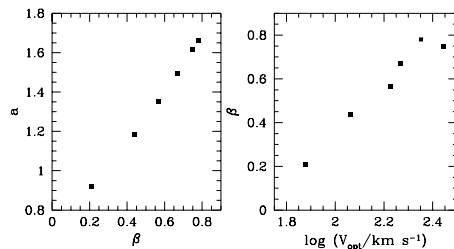


**Fig. 2.**  $a$  vs.  $\beta$  and  $\beta$  vs.  $V_{opt}$ .

profile that, out to  $r_{opt}$ , is *neutral* with respect to various different galaxy mass models:

$$V_{h,URC}^2(x) = V_{opt}^2 (1 - \beta) (1 + a^2) \frac{x^2}{(x^2 + a^2)} \quad (3)$$

where  $x \equiv r/r_{opt}$ ,  $a$  the halo core radius in units of  $r_{opt}$  and  $\beta \equiv (V_{d,URC}/V_{opt})^2$  at  $R_{opt}$ . Then, by varying  $\beta$  and  $a$ ,  $V_{h,URC}$  can reproduce the maximum-disk, the solid-body, the no-halo, the all-halo, the NFW mass models. (e.g. CDM halos with concentration parameter  $c = 5$  and  $r_s = r_{opt}$  are well fit by (3) with  $a \simeq 0.33$ ) *iii*) by means of a number of high-quality high-resolution individual RC's [1] leading to trustworthy mass distributions. Let us define hereafter  $r_d$  as the disk scale-length and  $V_{opt} \equiv V(r_{opt})$ .

## 2 Dark Halos Properties from the Universal Rotation Curve

Let us remind the observational framework: *a*) the mass in spirals is distributed according to the Inner Baryon Dominance (IBD) regime [16]: there exists a characteristic transition radius  $r_{IBD} \simeq 2r_d(V_{opt}/220 \text{ km/s})^{1.2}$  for which, at  $r \leq r_{IBD}$ , the luminous matter completely accounts for the gravitating mass, whereas, at  $r > r_{IBD}$ , the dark matter shows up in the kinematics and *rapidly* becomes the dominant mass component [20, 18, 1]. Then, although dark halos extend down to the galaxy centers, it is only for  $r > r_{IBD}$  that they give non-negligible contributions to the circular velocity. *b*) DM is distributed in very differently way with respect to the baryons [16, 6], and *c*) the HI contribution to the circular velocity, at  $r < r_{opt}$ , is small [e.g. 17].

Persic, Salucci and Stel [16] have derived from  $\sim 20000$  velocity measurements, relative to  $\sim 900$  rotation curves,  $V_{syn}(\frac{r}{r_{opt}}; M_I)$ , the synthetic rotation velocities of spirals binned in intervals of magnitudes. Each individual RC's (see Fig. (1)) shows a variance, with respect to synthetic curves of the corresponding magnitude, smaller than observational errors: spirals sweep a very narrow locus in the RC- profile/amplitude/ luminosity space. Thus, as regard the average main properties of the DM distribution, eq (3) is equivalent to a large sample of individual objects.

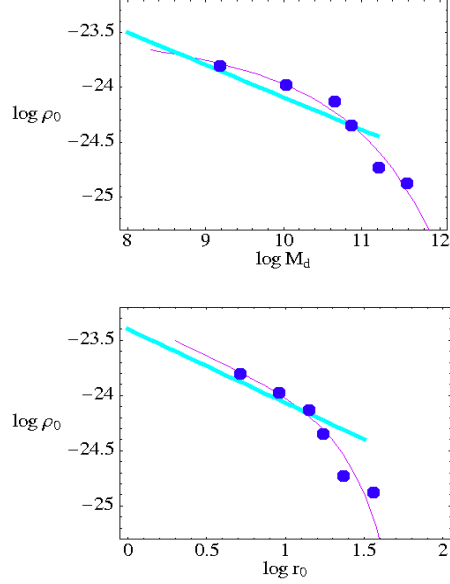


**Fig. 3.** *up)* Central halo density  $\rho_0$  (in  $\text{g}/\text{cm}^3$ ) *vs.* disk mass (in solar units) for normal spirals (*filled circles*); *bottom)* central density *vs.* core radii (in kpc) for normal spirals (see [19]).

The whole set of synthetic RC's define the Universal Rotation Curve (URC) that we represent analytically with the sum of two terms: *a)* the standard exponential thin disk term:

$$V_{d,URC}^2(x) = 1.28 \beta V_{opt}^2 x^2 (I_0 K_0 - I_1 K_1)|_{1.6x} \quad (4)$$

and the spherical halo term given by (3). The data (i.e. the synthetic curves  $V_{syn}$ ) select the actual mass model: by setting  $V_{URC}^2(x) = V_{h,URC}^2(x, \beta, a) + V_{d,URC}^2(x, \beta)$  with  $a$  and  $\beta$  as free parameters, an extremely good fit occurs when:  $\beta = \beta(\log V_{opt})$  and  $a = a(\beta)$  as plotted in Fig. (2): the URC reproduces  $V_{syn}(r)$  up to its *rms* (i.e. within 2%). Moreover, at a fixed luminosity, the  $1\sigma$  fitting uncertainties for  $a$  and  $\beta$  are lesser than 20%.

The emerging scenario is the following: inside  $r_{opt}$  smaller objects have larger dark-to-stellar matter :  $M_*/M_{vir} \simeq 0.2 (M_*/2 \times 10^{11} M_\odot)^j$  ( $j \sim 0.75$ ) [20]) and within *each* galaxy the dark mass increases with radius with a power-law exponent between 2 and 3.

This evidence calls for a cored Dark Matter density [3, 4, 1]. Then, we are allowed to pass from the "neutral" distribution of DM of eq (3) in which a "core" may appear in the *velocity* profile (i.e. in a quantity which is directly measured), to the much more specific mass distribution given by the Burkert *density* profile that forces a core radius into the NFW profile.

$$\rho_B(r) = \frac{\rho_0 r_0^3}{(r + r_0)(r^2 + r_0^2)} \quad (5)$$

with  $\rho_0$  and  $r_0$  free parameters (the central DM density and the core radius). Then  $M_B(r) = 4 M_0 \{ \ln(1 + r/r_0) - \arctan(r/r_0) + 0.5 \ln[1 + (r/r_0)^2] \}$  with  $M_0 \simeq 1.6 \rho_0 r_0^3$  the dark mass within  $r_0$ . The halo contribution to the circular velocity is:  $V_{h,B}^2(r) = G M_B(r)/r$ .

The Disk + Burkert halo model applied to the synthetic rotation curves leads to core parameters  $r_0$ ,  $\rho_0$  strong correlated and linked to the disk mass : dark halos behave as an 1-parameter family, completely specified by *e.g.* their central density  $\rho_0$  (see Fig. (3) ).

These relationships imply that the densest halos harbor the least massive disks (see Fig. 3) while the feature of the curvature at the highest masses/lowest densities in the  $\rho_0$  *vs.*  $r_0$  relationship may be related to the existence of an *upper mass limit* in  $M_{vir}$  at  $few \times 10^{12} M_\odot$ .

## 2.1 Testing CDM with the URC

From the analysis of the URC one concludes that dark halos are not kinematically cold structures, but “warm” regions of sizes  $r_0 \propto \rho_0^{-1.5}$  with  $r_0 \sim 4 - 7 r_d$ . Then, the boundary of the core region is beyond the region of the stellar disk. There is no evidence that the DM density converges to a  $r^{-1}$  (or a steeper) regime, as dictated by CDM scenario.

## 3 Dark Matter Properties from Individual Rotation Curves

Although deriving halo densities from individual RC’s is certainly complicated, the belief according to which one is bound to get ambiguous halo mass modeling [as claimed in some work] is not always correct. In fact, this is true only for rotation curves of low spatial resolution, i.e. those with less than  $\sim 3$  measures per exponential disk length-scale, as most of HI rotation curves. In this case, since the parameters of the galaxy structure are crucially sensitive to the *shape* of the rotation curve in the region  $0 < r < r_d$ , there are no sufficient data to constrain the mass model. In the case of high-quality *optical* RC’s tens of independent measurements solve the problem. Moreover, since the dark component can be better traced when the disk contributes to the dynamics in a modest way, a convenient strategy leads to investigate DM-dominated objects, like dwarf and low surface brightness (LSB) galaxies. For the latter [e.g. 7, 11, 3, 4, 9, 10, 21, 23] the results are not definitive in that they unfortunately are intrinsically uncertain, due to the limited quality of their kinematics.

Since the observed RC’s have Universal features and most of the properties of cosmological halos are also claimed universal, an useful strategy is to investigate a restricted number of high-quality *optical* rotation curves of *low luminosity* late-type spirals, with *I*-band absolute magnitudes  $-21.4 < M_I < -20.0$  and  $100 < V_{opt} < 170 \text{ km s}^{-1}$ . Objects in this luminosity/velocity range are DM dominated [e.g. 20] but their optical RC’s, measured at a typical angular resolution of  $2''$ ,

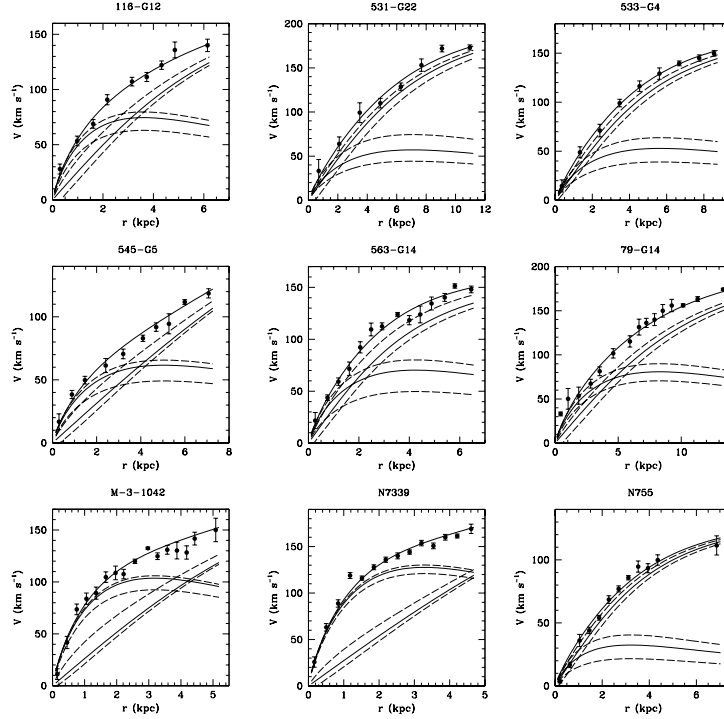


**Fig. 4.** B+ Disk models (*thick solid line*) (*points with errorbars*). Thin solid lines represent the disk and halo contributions. The maximum and minimum disk solutions (*dashed lines*) provide the uncertainties see [1]

have the excellent spatial resolution of  $\sim 100(D/10 \text{ Mpc}) \text{ pc}$  and  $n_{\text{data}} \sim r_{\text{opt}}/w$  independent measurements. For nearby galaxies:  $w \ll r_d$  and  $n_{\text{data}} > 25$ .

In [1] we extracted, from the ‘excellent’ subsample of 80 rotation curves of [15], the best 9 rotation curves. These RC’s (as any rotation curve that candidates itself to yield something crucial on the DM distribution) trace properly the gravitational potential since satisfy the following quality requirements: 1) data extend at least out to the optical radius, 2) they are smooth and symmetric, 3) they have small internal *rms*, 4) they have high spatial resolution and a homogeneous radial data coverage of 30 – 100 data points between the two arms. Each RC has 7 – 15 velocity points inside  $r_{\text{opt}}$ , each one being the average of 2 – 6 independent data. The RC’s spatial resolution is better than  $1/20 r_{\text{opt}}$ , the velocity *rms* is about 3% and the RC’s logarithmic derivative is generally known within about 0.05.

We model the mass distribution as the sum of two components: a stellar disk and a spherical dark halo, therefore:  $V^2(\text{observed}) = V^2(\text{disk}) + V_h^2(\text{halo})$ . Light traces the stellar mass via the radially constant mass-to-light ratio. We neglect the gas contribution  $V_{\text{gas}}(r)$  since in normal spirals it is small [17, Fig. 4.13]:  $\beta_{\text{gas}} \equiv (V_{\text{gas}}^2/V^2)_{r_{\text{opt}}} \sim 0.1$ . Incidentally, this is not the case for dwarfs

and LSBs: most of their kinematics is affected in different ways by the HI disk gravitational pull. The disk contribution to circular velocity is given by (4), while the dark halo contribution by (3). Finally we normalize (at  $r_{opt}$ ) the velocity model  $(V_d^2 + V_h^2)^{1/2}$  to the observed rotation speed  $V_{opt}$ .

For each galaxy, we determine the values of the parameters  $\beta$  and  $a$  by means of a  $\chi^2$ -minimization fit to the observed rotation curves:

$$V_{model}^2(r; \beta, a) = V_d^2(r; \beta) + V_h^2(r; \beta, a) \quad (6)$$

A central role in performing the mass decomposition is played by the derivative of the velocity field  $dV/dr$ . It has been shown [e.g. 14] that by taking into account the logarithmic gradient of the circular velocity field defined as:  $\nabla(r) \equiv \frac{d \log V(r)}{d \log r}$  one best retrieves the crucial information stored in the shape of the rotation curve. Then, we set the  $\chi^2$  statistics as the sum of  $\chi^2$ 's evaluated on velocities and on logarithmic gradients. In detail, by setting  $\chi_V^2 = \sum_{i=1}^{n_V} \frac{V_i - V_{model}(r_i; \beta, a)}{\delta V_i}$  and  $\chi_{\nabla}^2 = \sum_{i=1}^{n_{\nabla}} \frac{\nabla(r_i) - \nabla_{model}(r_i; \beta, a)}{\delta \nabla_i}$ , we minimize the quantity

$$\chi_{tot}^2 \equiv \chi_V^2 + \chi_{\nabla}^2 \quad (7)$$

to get the mass model.

Let me point out that any claim of "different mass models" that all would account for a certain rotation curve, does instead originate from the (low) quality of the latter that does not allow a reasonably accurate derivation of  $\nabla(r)$ .

The best-fit models parameters for the "neutral" distribution of (3) are shown in Fig. 4. The disk-contribution  $\beta$  and the halo core radius  $a$  span a range from 0.1 to 0.5 and from 0.8 to 2.5, respectively. They are pretty well constrained in a small and continuous region of the  $(a, \beta)$  space. It is obvious that the halo curves are increasing almost linearly, out to the last data point. Remarkably, we find that the size of the halo density core is always greater than the disk characteristic scale-length  $r_d$  and it can extend beyond the disk edge (and the region investigated).

### 3.1 Testing CDM

Let us assume for the dark halos the NFW functional form given by (1) and fit the 9 RC's leaving  $c$  and  $r_s$  as free independent parameters, although N-body simulations and semi-analytic investigations indicate that they correlate in order to increase the chance of a good fit. It must be assumed, however, for these 9 test objects, a conservative halo mass upper limit of  $2 \times 10^{12} M_{\odot}$ . The fits to the data are shown in Figs. (5) and (6), together with the URC fits: for seven out of nine objects the NFW models are unacceptably worse than the URC solutions. Moreover, the resulting CDM disk  $I$ -band mass-to-light ratios turn out to be in some cases  $\sim 0.01$  solar units, i.e. unacceptably low in the  $I$ -band.

We definitely conclude that there is no shortage of dark halos around objects with a trustable rotation curve, that show a density distribution inconsistent with that predicted by collision-less CDM.

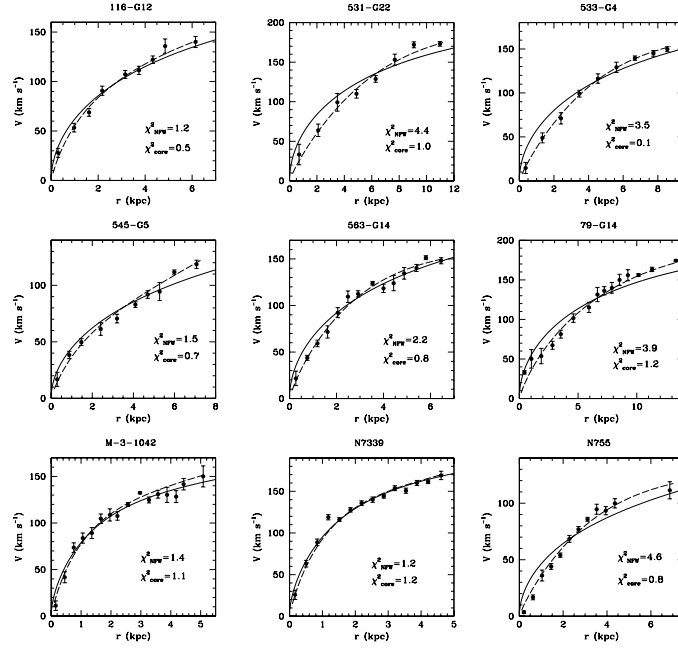


**Fig. 5.** NFW best-fits *solid lines* of the rotation curves (*filled circles*) compared with the URC halo + Disk fits (*dashed lines*). The  $\chi^2$  values are also indicated.

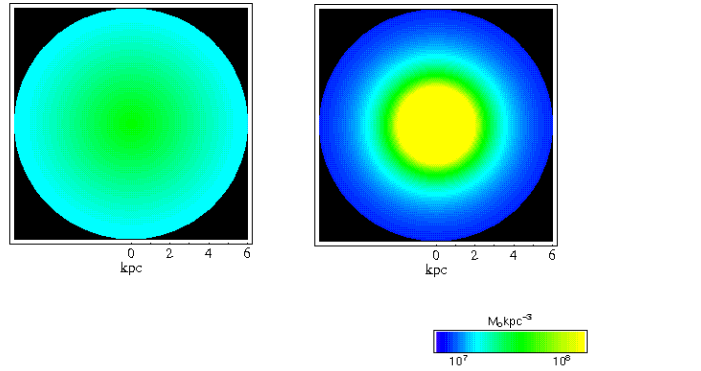


**Fig. 6.** *left*) The density of the dark halo of 116-G12, *right*) The CDM prediction

## 4 Halos around Ellipticals

The very low scatter that ellipticals show lying on the Fundamental Plane is a kinematical feature that can be used to investigate their Dark Matter distribution. The central velocity dispersion  $\sigma_0$  is the key quantity, in that it strongly de-



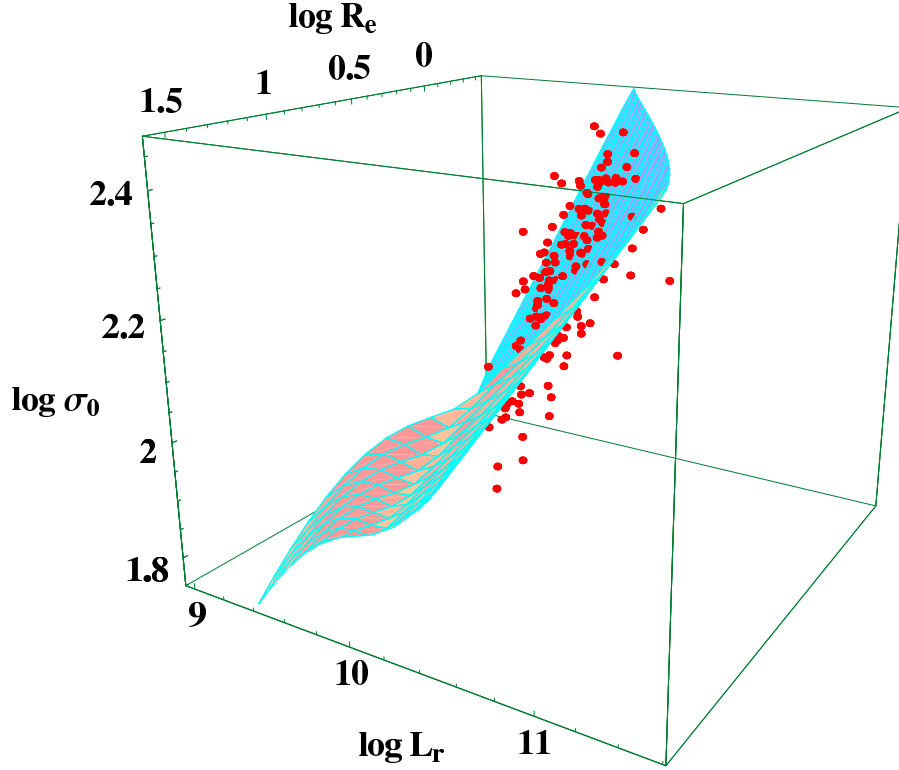


**Fig. 7.** The CDM surface in the log-space  $(R_e, L_r, \sigma_0)$  compared to sample data (points).  $R_e$  in kpc,  $L_r$  in  $L_{r\odot}$  and  $\sigma_0$  in km/s.

depends on the mass distribution of both stellar and dark matter [34]. A sample of 221 E/S0 galaxies with good photometric and spectroscopic data has been used to investigate this point. This sample defines the standard "empirical" FP in the coordinate space of  $(\log \sigma_0, \log R_e, \log L_r)$ . The galaxies have an average distance of 0.084 dex with respect to the plane, of the order of the measurement uncertainties, estimated as large as  $\pm 0.05$  dex.

It is easy to show, for the NFW distribution of  $\Lambda$ CDM cosmology, that  $\sigma_0$  is a specific function of the total virial mass and the stellar mass-to-light ratio, with no other free parameters. For the Burkert (1995) density distribution,  $\sigma_0$  depends instead on the stellar mass-to-light ratio, the value of the core radius  $r_0$  and the fraction of dark mass inside  $R_e$ .

It is shown that the existence of a tight FP relating the above quantities implies that ellipticals are largely dominated, within  $R_e$ , by the stellar spheroid, independently of the actual DM distribution. However,  $\Lambda$ CDM predicts large amounts of dark matter inside  $R_e$  in view of the cuspy density distribution of

CDM halos: as results in this framework the ellipticals would lie on a curved surface, inconsistent with the observed *plane* (see Fig. (7)).

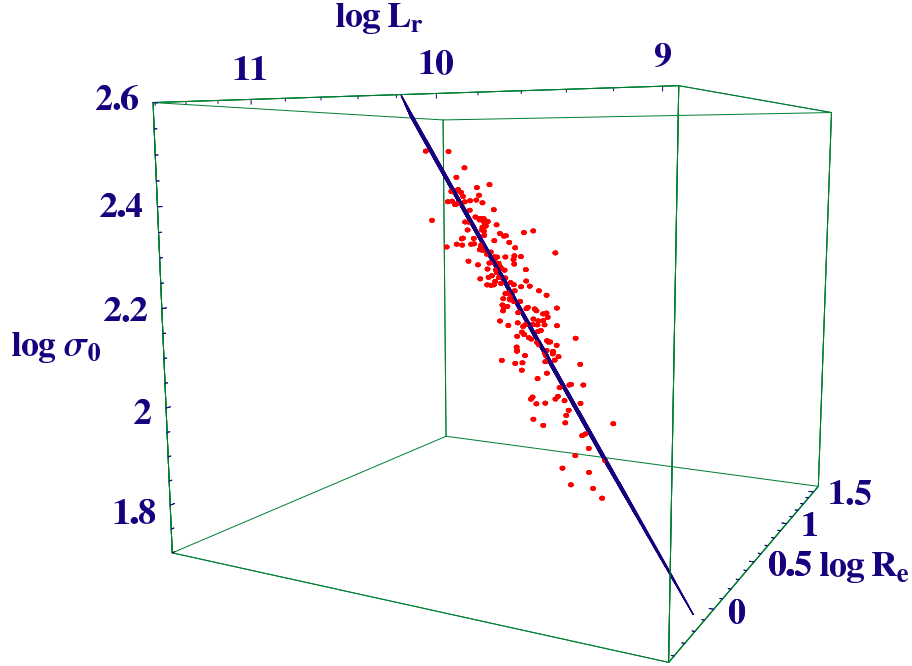


**Fig. 8.** The plane from Spheroid+Burkert halo model.

The Burkert density distribution, in which substantial amounts dark matter can be placed outside  $R_e$ , leads to a relationship that is a plane resulting in perfect agreement with the observed one (see Fig (8)). This implies a dark-to-luminous mass fraction within the effective radius of about  $0.3 \pm 0.2$  and a luminosity dependence of the spheroidal mass-to-light ratio:  $M_{sph}/L_r = (5.3 \pm 0.1)(L_r/L_{*r})^{0.21 \pm 0.03}$ , in Gunn- $r$  band. Moreover, as a firm constraint, we can state  $r_0 > R_e$ .

## 5 More Support for Core Radii.

The Trieste group has provided a crucial evidence on the "core radii" issue, however, results from other investigations are also very important and must be considered, in that, alongside with those referred in the previous sections, build a formidable case for the existence of constant density cores at the centers of the dark halos surrounding spiral galaxies.

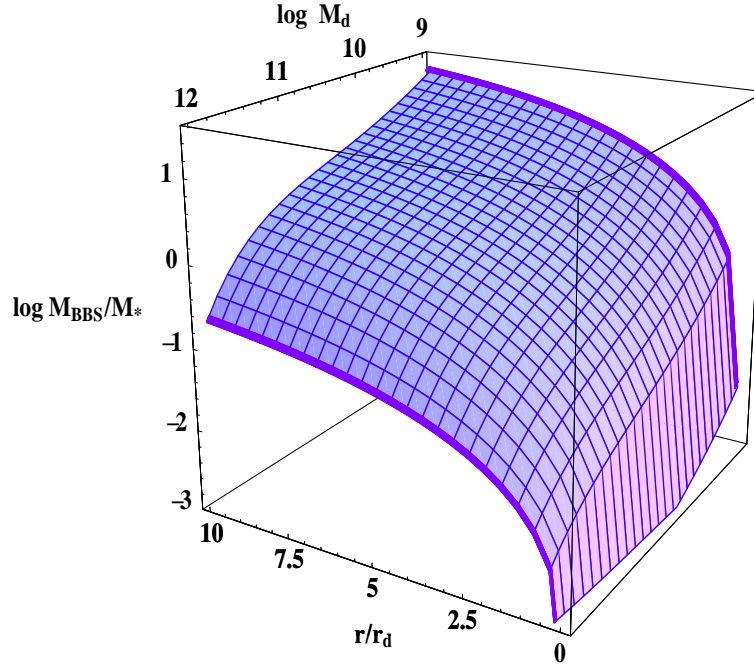


**Fig. 9.** The dark-to-luminous mass ratio as function of the normalized radius and the total disk mass. BBS halo is the Burkert profile as in Borriello and Salucci [1]

**Table 1.** Extra Evidence

Author(s)	Paper
Ortwin et al	AJ 121, 1936
Fuchs	astro-ph/0212485
Swaters et al .	ApJ 583, 732
Weldrake et al.	MN 340, 12
Bottema &	Verheijen A&A 388, 793
Bolatto et al.	ApJ 565, 238
de Blok et al.	AJ 122, 2396
de Blok et al.	ApJL 552, 23
Stil & Israel	A&A 392, 473
Dutton et al.	astro-ph/0310001
Marchesini et al.	ApJ. 575, 801
Fraternali et al.	AJ 123, 3124

## 6 The Intriguing Evidence from Dark Matter Halos

From observations the dark halos around galaxies emerge as an one-parameter family; the order parameter (either the central density or the core radius) corre-

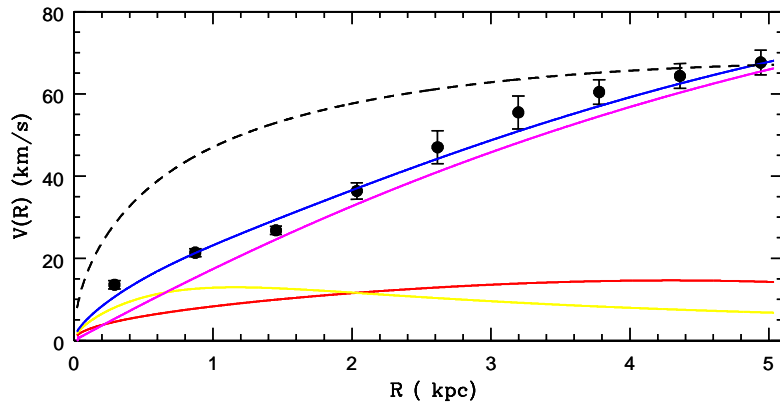


**Fig. 10.** DDO 47 rotation curve vs different mass models. The continuous line is the sum of the stellar (red), the gas (yellow) and the Burkert halo distributions (magenta). The dashed line represents the NFW distribution.

lates with the stellar mass. However, the global structural properties of the dark halo, like the virial radius or the virial mass could be extrapolated only empirically, because we do not know how to prolongate, outside the region mapped by data and in a theoretical way, the DM profile. In fact, inside the stellar disk region, the halo RCs are determined by physical parameters, the central core density and the core radius, that have no counterpart in the gravitational instability/hierarchical clustering picture.

Important relationships among physical quantities still emerge from the mass modelling: in Fig. 9 we show the dark-to-luminous mass ratio as function of the normalized radius and of the total disk mass. The surface has been obtained by adopting the correlations between the halo and the disk parameters derived in [19]. Therefore the dark-to-stellar mass ratio, at fixed fraction of disk length-scales, increases as the total disk mass decreases; for example: in the range  $1 < r/r_d \leq 3$  it raises by 20% for massive disks ( $M_d = 10^{12} M_\odot$ ) while it raises by 220% for smaller disks ( $M_d = 10^9 M_\odot$ ).

Two conclusive statements can be drawn: dark matter halos have an inner constant-density region, whose size exceeds the stellar disk length-scale. Second, there is no evidence that dark halos converge, at large radii, to a  $\rho \sim r^{-2}$  (or steeper) profile.

The existence of a region of “constant” density as wide as the stellar disk is hardly explained within current theories of galaxy formation. A number of different solutions have been proposed to solve this problem [e.g. 30, 31, 32, 33]. Before commenting on them let us stress that any solution of the “core radius” issue must account for all the intriguing halo properties described in this review. Let us point out that we review the several tenths of attempts for a solution

to the "core radii" issue will be reviewed elsewhere. Here we just classify them in families:

- 1- Dark Matter "interacted" with itself or with baryons. Original "cuspy" halos have been smoothed in this way.
- 2- Dark Matter has a different power spectrum/perturbations evolution than the current Standard Picture and this has "produced" the cores.
- 3- Dark Matter is a "field", that naturally mimicks the effects of a cored halo of particles.
- 4- Within the standard  $\Lambda$ CDM scenario, N-Body simulations have failed, for a variety of reasons, to discover this intrinsic and real feature.

## 7 Prologue

Let me finish where I started: i.e. by showing a test case for the existence of a core in the density distribution of the dark halo around a galaxy. DDO 47, see Fig (10) has a rotation curve that increases linearly from the first data point, at 300  $pc$ , up to the last one, at 5  $kpc$  well beyond the stellar disk edge. The RC profile implies the presence of a dominating (dark) halo with an (approximately) constant density out to the last measured point, *prior* any mass modelling.

## 8 Acknowledgments

P.S thanks G. Danese for stimulating discussions and I. Yegorova for help in the presentation.

## References

1. A. Borriello, P. Salucci: MNRAS, **323**, 285 (2001)
2. J.S. Bullock, T.S. Kolatt, Y. Sigad, R.S. Somerville, A.V. Kravtsov, A.A. Klypin, J.R. Primack, A. Dekel: MNRAS, **321**, 559 (2001)
3. A. Burkert: ApJ, **447**, L25 (1995)
4. A. Burkert, J. Silk: ApJ, **488**, L55 (1997)
5. S. Cole, C. Lacey: MNRAS, **281**, 716 (1997)
6. E. Corbelli, P. Salucci: MNRAS, **311**, 411C (2000)
7. R. Flores, J.R. Primack: ApJ, **427**, L1 (1994)
8. T. Fukushige, J. Makino: ApJ, **477**, L9 (1997)
9. A.V. Kravtsov, A.A. Klypin, J.S. Bullock, J.R. Primack: ApJ, **502**, 48 (1998)
10. S.S. McGaugh, W.J.G. de Blok: ApJ, **499**, 41 (1998)
11. B. Moore: Nature, **370**, 629 (1994)
12. B. Moore, F. Governato, T. Quinn, J. Stadel, G. Lake: ApJ, **499**, L5 (1998)
13. J.F. Navarro, C.S. Frenk, S.D.M. White: ApJ, **462**, 563 (1996)
14. M. Persic, P. Salucci: MNRAS, **245**, 577 (1990b)
15. M. Persic, P. Salucci: ApJS, **99**, 501 (1995)
16. M. Persic, P. Salucci, F. Stel: MNRAS, **281**, 27P (1996)
17. M.-H. Rhee: PhD thesis, Groningen University (1996)
18. P. Salucci, C. Ratnam, P. Monaco, L. Danese: MNRAS, **317**, 488S (2000)
19. P. Salucci, A. Burkert: ApJ, **537L**, 9S (2000)
20. P. Salucci, M. Persic: MNRAS, **309**, 923 (1999)
21. J. Stil: Ph.D. Thesis, Leiden University (1999)
22. T.S. van Albada, J.S. Bahcall, K. Begeman, R. Sancisi: ApJ, **295**, 305 (1985)
23. F.C. van den Bosch, B.E. Robertson, J. Dalcanton, W.J.G. de Blok: AJ, **119**, 1579V (2000)
24. M. Persic, P. Salucci: in *Dark and Visible Matter in Galaxies*, ASP Conf. Ser., **117**, ed. Persic & Salucci (1997)
25. P. Salucci, A. Burkert: ApJ, **537**, L9 (2000)
26. W.J.G. de Blok, S. S. McGaugh, A. Bosma, V. C. Rubin: ApJ, **552**, 23 (2001)
27. C. M. Trott, R. L. Webs: astro-ph/0203196, *in press* (2002)
28. L. D. Matthews, J. S. Gallagher, III: astro-ph/0203188, *in press* (2002)
29. S. Blais-Ouellette, C. Carignan, P. Amram: astro-ph/0203146 to be published in: *Galaxies: the Third Dimension*, ASP Conf. Ser. (2002)
30. M. White, R.A.C. Croft: AJ, **539**, 497 (2000)
31. P.J.E. Peebles: ApJ, **534**, 127 (2000)
32. C. Firmani, E. D'Onghia, V. Avila-Reese, G. Chincarini, X. Hernandez: MNRAS, **315**, 29 (2000)
33. A. El-Zant, I. Shlosman, Y. Hoffman: ApJ, **560**, 636 (2001)
34. A. Borriello, P. Salucci, L. Danese: MNRAS **341**, 1109 (2003)